Spin reorientation and glassy dynamics in $La_{1.55}Sr_{0.45}NiO_4$

S. R. Giblin*
ISIS Facility, Rutherford Appleton Laboratory, Chilton, Didcot, Oxon OX11 0QX, United Kingdom

P. G. Freeman
Institute Laue-Langevin, Boîte Postale 156, 38042 Grenoble Cedex 9, France

K. Hradil
Institut für Physikalische Chemie, Universität Göttingen, Tammanstrasse 6, 37077 Göttingen, Germany

D. Prabhakaran and A. T. Boothroyd
Department of Physics, Oxford University, Oxford OX1 3PU, United Kingdom
(Received 24 June 2008; revised manuscript received 15 September 2008; published 19 November 2008)

The magnetism of charge-stripe-ordered $La_{1.55}Sr_{0.45}NiO_4$ was studied by a combination of neutron diffraction, muon-spin relaxation (μSR), and bulk susceptibility. Long-range magnetic ordering was observed at a lower temperature by μSR than by neutron diffraction, consistent with a glassy transition to the ordered phase. A second magnetic transition is detected by all techniques and is consistent with a spin reorientation. On cooling below $T_{SR}=42$ K the spins reorientate from lying $32.9\pm0.6°$ away from the stripe direction at 70 K to $56.8\pm0.4°$ at 10 K. The magnetic order was observed by neutron diffraction to have both three-dimensional and two-dimensional (without any correlation along the c axis) characters. μSR measurements confirmed this and are consistent with a single magnetically ordered spin-stripe phase. The effects of checkerboard charge order on the ordered phase and the characteristics of the phase diagram of the spin reorientation in charge-ordered $La_{2-x}Sr_xNiO_4$ are commented on.

DOI: 10.1103/PhysRevB.78.184423 PACS number(s): 71.27.+a, 75.25.+z, 76.75.+i

I. INTRODUCTION

The behavior of charge-ordering (CO) and spin-ordering (SO) phenomena in doped transition-metal oxides has provided a wealth of opportunity for researchers. In particular this work has stemmed from the original observation of incommensurate magnetic fluctuations observed in superconducting $La_{2-x}Sr_xCuO_4$ (LSCO).[1,2] Resultant investigation concluded this behavior to be consistent with charge-stripe correlations.[3] Specifically, magnetic fluctuations in the superconducting state of LSCO have been shown to be centered on wave vectors parallel to Cu-O bonds.[4] These fluctuations rotate to 45° to the Cu-O bond in the nonsuperconducting phase.[5] $La_{2-x}Sr_xNiO_4$ (LSNO) is known to be isostructural with LSCO. However superconductivity is not observed; both materials exhibit a spin-charge-ordered "stripe" phase[3,6] in their rich respective phase diagrams. This makes LSNO an ideal material in which to examine the phenomena of stripe ordering without the complications of superconductivity.

Charge-stripe ordering in LSNO has previously been investigated using neutrons[7–13] and x rays.[14–16] Despite a number of investigations into the charge-stripe structure, only the crystal structure has been experimentally determined.[17] A complete structural determination of the charge- and spin-stripe structures in these materials has yet to be obtained. In addition to diffraction measurements, probes such as Raman[18] and infrared[19] spectroscopies observe a symmetry change consistent with charge-stripe ordering in LSNO. The charge stripes are observed from diffraction measurements to be static on the relative experimental time scales, and correlations in excess of 100 Å have been observed for certain compositions.[8–10] This indicates a degree of stability in the spin-stripe structure that forms below the charge-stripe-ordering temperature. However neutron-diffraction experiments have indicated a spin reorientation (SR) below the ordering temperature for long-range two-dimensional (2D) antiferromagnetic spin stripes in the compositional range $0.275\leq x\leq 0.5$,[11,12,20] highlighting an inherent instability in the stripe systems. The SR temperature occurs at higher temperatures for both the $x=0.33$ and 0.5 LSNO samples and has been attributed to a commensurability that pins the charges to the lattice.[11,20] The $x=0.5$ has a highly stable checkerboard charge-ordered state.[6,10] All samples that demonstrate a SR have also been shown to exhibit remnant magnetization, indicative of glasslike behavior. Moreover there is a dramatic change in the functional form of the remnant magnetization around the SR temperature.[13]

The purpose of this work is to further characterize the compositional doping levels up to $x=0.5$, more specifically to investigate the stability of the spin stripes as the checkerboard-type order, obtained at half doping, is approached from lower doping levels. At half doping the magnetic excitation spectrum of LSNO shows additional modes to those observed at $x\sim 1/3$.[21] To correctly understand the magnetic excitation spectrum below half doping, the magnetic structure of this material must be determined. This investigation will concentrate on the $La_{1.55}Sr_{0.45}NiO_4$ composition, which may determine if the base-temperature spin orientation correlates with the charge-ordering temperature as previously postulated, or whether the increase in Sr doping increases a strain effect in the lattice producing a favored orientation.[12] The $x=0.45$ composition has both incommensurate charge- and spin-stripe orderings. From this investigation it can be determined if the enhancement of the spin

reorientation in the half-doped LSNO is due to the occurrence of the highly stable commensurate checkerboard charge-ordered state.

Using standard neutron-scattering techniques, the SR temperature in the $x=0.45$ is observed to be enhanced with respect to other incommensurate doping compositions. The enhancement occurs as the half-doping composition is approached even though the spin and charge stripes are *not commensurate* with the lattice. The magnetic neutron scattering is characterized by both 2D and three-dimensional (3D) magnetic peaks, indicating two components to the magnetic order. The magnetic frustration is characterized using standard volume-averaged magnetometry techniques and probed directly on a microscopic scale using muon-spin rotation (μSR). The muon is shown to act as a passive probe of the SR and detects no behavior consistent with long-range glassy phenomena in the microsecond time scale. Glassy behavior observed in the susceptibility measurements cannot be viewed as a spin glass. However the μSR clearly demonstrates evidence of competing magnetic interactions. The magnetic ordering is observed to occur at a lower temperature in μSR than in neutron diffraction, indicating that the transition to the magnetically ordered state is glassy and results from a slowing down of fluctuating magnetic correlations. Moreover the muons clearly demonstrate that the sample is a single magnetic phase, which is important when considering the interpretation of the neutron results.

II. EXPERIMENTAL

Single crystals of $La_{1.55}Sr_{0.45}NiO_4$ were grown using the floating-zone technique.[22] All samples used were cut from the same crystal ingot, a rod of 6 mm in diameter. Initial magnetic characterization of the sample was performed on a Quantum Design MPMS XL superconducting quantum interference device (SQUID) magnetometer with the susceptibility recorded parallel and perpendicular to the *ab* plane. All measurements were performed using the standard zero-field-cooled (ZFC) and field-cooled (FC) protocols in a measuring field of 10 mT.

Unpolarized- and polarized-neutron-diffraction measurements were performed on the triple-axis spectrometers PUMA at FRM-II and IN20 and IN3 at the Institut Laue-Langevin. The data were collected with a fixed incident and final neutron wave vector of $k_f=2.662$ Å. A pyrolytic graphite (PG) filter was placed after the sample to suppress higher-order harmonic scattering. The energies of the incident and scattered neutrons were selected by Bragg reflection from a double-focusing PG crystal monochromator on PUMA, a vertically focused PG crystal monochromator on IN3, and an array of Heusler crystals on IN20. On IN3 the neutron beam was collimated by 60 min before and after the sample position. For polarized-neutron scattering on IN20, the spin polarization **P** was maintained in a specified orientation with respect to the neutron wave vector **Q** using an adjustable guide field of a few milliteslas at the sample position. The sample was orientated so that on PUMA $(h,k,0)$ positions and on IN20 and IN3 (h,h,l) positions in reciprocal space could be accessed. LSNO has a tetragonal unit cell, with the

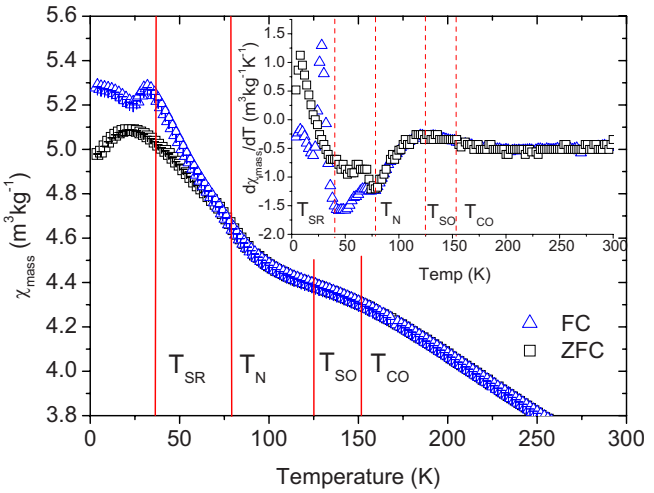

FIG. 1. (Color online) The temperature dependences of the magnetic susceptibility for both the FC and ZFC protocols. The measuring field in both cases was 10 mT and applied parallel to the *ab* plane. The charge order and spin order obtained from neutron scattering are indicated. The inset shows the derivative of the mass susceptibility with respect to temperature. The temperature labels are described in the text.

cell parameters $a\approx3.8$ Å and $c\approx12.7$ Å. The correlation lengths stated in this paper are resolution corrected from the widths of the structural Bragg reflections.

μSR measurements were performed in zero field (ZF) on the Dolly spectrometer at the PSI in Switzerland. Muons are fundamental spin-1/2 particles, and are implanted randomly into the sample to act as a microscopic probe of bulk magnetic properties. The subsequent decay of the muon into a positron is dependent on the final spin direction of the muon, enabling the internal fields to be mapped out with respect to the muon implantation sites.

III. RESULTS

Figure 1 shows the temperature dependence of the magnetic susceptibility for both the FC and ZFC data when the field is applied in a direction parallel to the *ab* plane. The general form of the susceptibility is similar to that of other compositions.[13] A change in the slope of the susceptibility corresponds to a CO (Ref. 12) at high temperatures and a resultant SO at lower temperatures. $x=0.45$ has a CO temperature of 150 K with the SO on the neutron time scale occurring at 125 K. These are observed as a subtle change in the derivative of the mass susceptibility as shown in the inset of Fig. 1.

Magnetic frustration can be clearly identified in the derivative of the mass susceptibility with respect to the temperature. The irreversibility point is clearly highlighted in the inset of Fig. 1 as a difference between the FC and ZFC data at 78 K (T_N). The occurrence of long-range magnetic order and the observation of spin frustration is an unresolved problem of LSNO, for which possible scenarios have previously been discussed.[13] Finite domain size, finite-length charge stripes, or competing length scales of the Coulomb and mag-

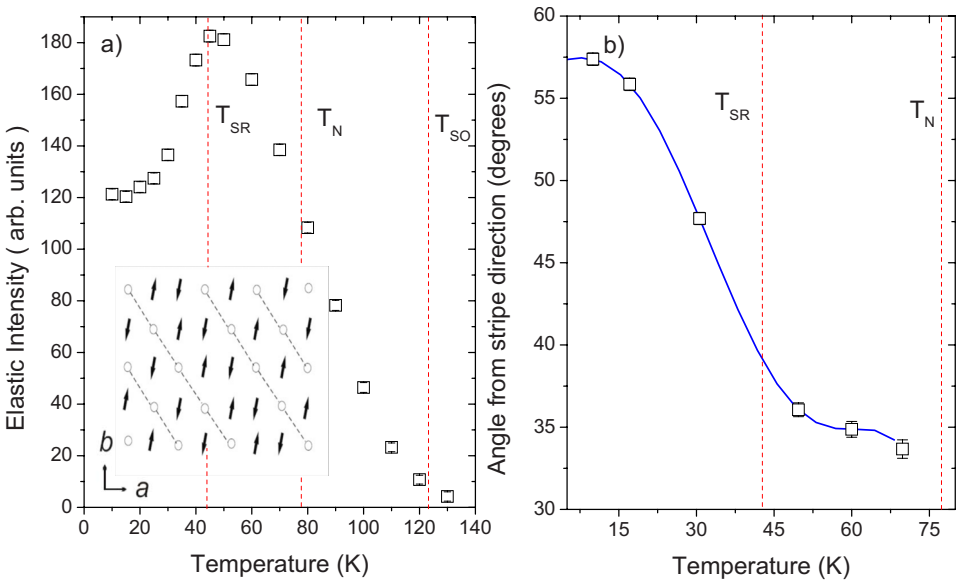

FIG. 2. (Color online) (a) The temperature dependence of the intensity of the magnetic Bragg peak at $\mathbf{Q_2}=(0.71,0.71,0)$; the SR occurs at 42.5 K. The inset demonstrates the spin-charge ordering in $La_{1.55}Sr_{0.45}NiO_4$, where arrows denote the Ni^{2+} ions and circles denote the holes. (b) The temperature dependence of the angle from the stripe direction of the Ni^{2+} ions. The line is a guide for the eyes.

netic interactions are different explanations for this dual character that are consistent with the present understanding of LSNO.[13,23] Magnetic order accompanied by spin frustration is also observed in the "spin-glass" phase[24,25] of magnetically "charge-stripe-ordered" cuprates.[26,27] μSR measurements reveal that these materials are magnetically ordered on the time scale of microseconds,[26,27] with bulk magnetization measurements indicating spin frustration observed as FC and ZFC splittings.[25] In the cuprates as in charge-stripe-ordered LSNO, there is bulk magnetic order throughout the material and observed spin frustration.

Below the spin ordering in $x=0.45$ LSNO, the magnetic stripes have not stabilized, resulting in an upturn in the derivative of both the FC and ZFC data at 42 K (T_{SR}) seen in the inset of Fig. 1. Note that no evidence of a ZFC/FC splitting and hence a glassy transition is observed when the measuring field is applied perpendicular to the *ab* plane (not shown), indicating the sensitivity of the effects to field direction.

Neutron diffraction and magnetic susceptibility probe in different time domains. dc susceptibility is essentially a static probe, whereas neutron scattering provides a snapshot of the magnetic correlations on a time scale of 10^{-12} s. This could in part explain why the spin- and charge-ordering temperatures observed by neutron diffraction correspond only to very subtle features in the bulk susceptibility, and why an extra apparently frustrated transition is also observed in the susceptibility measurements.

Charge-stripe order in LSNO results in magnetic Bragg reflections at $(h+1/2\pm\varepsilon/2,k+1/2\pm\varepsilon/2,l)$ and superstructure Bragg reflections associated with the charge order at $(h\pm\varepsilon,k\pm\varepsilon,l)$, where h, k, and l are integers and ε is known as the incommensurability. The incommensurability varies with doping as $\varepsilon\sim x$, but with systematic deviations away from $\varepsilon=x$.[8] For $\varepsilon=1/3$ the charge-stripe order is said to be commensurate as the charge stripes are three lattice sites apart; for other values of ε the charge order is said to be incommensurate. For LSNO with $x=1/3$ and 1/2 magnetic Bragg peaks are only observed when l is an odd integer, but for other compositions magnetic Bragg peaks are observed at both odd and even l. In this study of $La_{1.55}Sr_{0.45}NiO_4$, peaks are observed at the expected magnetic- and charge-order positions for stripe-ordered LSNO with $\varepsilon=0.425$, consistent with previous studies of LSNO.[8,10] The inset of Fig. 2(a) shows the basic stripe pattern expected for $La_{1.55}Sr_{0.45}NiO_4$, assuming the stripes are centered on the Ni sites (site centered).[8] The arrows represent $S=1$ Ni^{2+} ions; the charge stripes are represented by open circles.

In Fig. 2(a) the temperature dependence of the integrated intensity of the magnetic Bragg reflection at $\mathbf{Q_2}=(0.71,0.71,0)$ is shown, retaining the labeling in previous work.[11,12] This reflection arises from domains in which the charge stripes run parallel to $[1\bar{1}0]$ as shown in the inset of Fig. 2(a). Since magnetic neutron diffraction is sensitive to spin components perpendicular to $\mathbf{Q}$, the scattering at $\mathbf{Q_2}$ comes mainly from the spin components parallel to the stripe direction and along the *c* axis, the latter of which is found to be zero[11,12,20] as expected given the easy-plane *xy*-like anisotropy in LSNO. Figure 2(a) shows that on cooling the magnetic Bragg reflection increases from zero intensity at 130 K, and reaches a maximum at 50 K as the ordered moment increases in magnitude. On further cooling below $T_{SR}=42.5\pm2.5$ K,[28] the intensity of the reflection decreases, implying that the component parallel to the stripe direction decreases, consistent with a SR away from the stripe direction.

By employing *XYZ* longitudinal polarization analysis neutron diffraction, it is possible to determine the angle[11] ϕ that the ordered Ni^{2+} ions are directed away from the stripe direction; e.g., for $\phi=90°$ the spins are aligned perpendicular to the direction of the stripes. The two magnetic Bragg reflections chosen for this analysis were $\mathbf{Q_1}=(0.29,0.29,3)$ and $\mathbf{Q_2}=(0.71,0.71,1)$ so that $\mathbf{Q}_1$ and $\mathbf{Q}_2$ are directed close to $(0,0,l)$ and $(h,h,0)$, respectively. The scattering from $\mathbf{Q}_1$ arises mainly from the total in-plane spin moment, while that at $\mathbf{Q}_2$ comes mainly from the spin components parallel to the stripe direction and along the *c* axis as mentioned above. To analyze the direction of the spins over this temperature

range, the direction of the neutron polarization **P** was varied relative to the scattering vector **Q**.

From measurements at 10 and 60 K on $\mathbf{Q}_1$ and $\mathbf{Q}_2$, it was determined that the spins lie on the *ab* plane within the resolution of the technique. Assuming that the spins lie on the *ab* plane for the rest of the temperature range, $\mathbf{Q}_1$ is used to determine the spin orientation. This method is described in Ref. 20. Figure 2(b) shows the temperature dependence of this spin orientation. On cooling from 70 K the spin orientation remains fairly constant at ~35°, then between 50 and 20 K the spins rotate away from the stripe direction by over 20°. By 20 K the spin reorientation is nearing completion and the spins are orientated at $56.8 \pm 0.4°$ away from the stripe direction at 10 K. From an orientation of $32.9 \pm 0.6°$ at 70 K, the complete spin reorientation is $23.9 \pm 0.5°$.

On cooling, the spins rotate away from the stripe direction in the same fashion as other LSNO charge-ordered materials in the compositional range $0.275 \leq x \leq 0.5$.[12] The charge-ordering temperature of $x=0.45$ is ~150 K. This has been estimated from an inflection in the susceptibility as shown in Fig. 1. Although the CO is not measured directly with neutrons in this experiment, the behavior of the susceptibility is consistent with other compositions measured using neutrons and susceptibility.[12] The SR in $x=0.45$ is at a temperature of ~50 K, similar for $x=1/3$ and 0.5, but unlike other incommensurately doped nickelates in which the SR occurs at ~15 K. This suggests that strict long-range commensurability is not required for a high SR temperature. The SR in $x=0.45$ is of the same magnitude as that in the $x=0.5$ ($26 \pm 5°$), and larger than the SR of $10° - 15°$ observed in the doping range $0.275 \leq x \leq 0.4$.

Correlation lengths were obtained from the spin-ordering peaks of $x=0.45$ from the inverse of the half-width at half maximum of the Bragg reflections. The l dependence of the magnetic scattering was measured with polarized-neutron scattering with $\mathbf{P} \| \mathbf{Q}$, a configuration where all the spin-flip (SF) scattering is magnetic in origin. Figure 3(a) shows a SF and a non-spin-flip (NSF) scan in the l direction passing through the magnetic Bragg reflection at (0.29,0.29,3). There is a peak at $l=3$, with a correlation length of 21.4 ± 0.7 Å, but no peak at $l=2$. However there are a large number of counts in the SF channel at $l=2$ when compared to the NSF channel, indicative of a strong magnetic background scattering that is l independent. For incommensurate charge-stripe-ordered LSNO, magnetic Bragg reflections occur at all l =integer, inconsistent with the lack of peak at $l=2$ in the $x=0.45$. The correlation parallel to the stripe direction was found to be 121 ± 6 Å in the $(h,k,0)$ plane.

Stimulated by the observed magnetic background in Fig. 3(a), Figs. 3(b) and 3(c) show scans parallel to $(h,h,0)$ at $l=3$ and $l=2$, respectively. In both scans magnetic peaks are clearly observed. The peak at $l=3$ is sharper with a correlation length of 186 ± 12 Å, compared with the peak at $l=2$, which has a correlation length of 92 ± 6 Å. At $l=3$ the magnetic Bragg peak has finite correlation lengths in all directions, while the feature at $l=2$ shows that the signal originates from a ridge of magnetic scattering with no l dependence, i.e., from magnetic order that is uncorrelated along c and is therefore two dimensional in character.

Further unpolarized measurements on IN3 indicates that the observed l-independent scattering occurs across the temperature range of 1.5–110 K. Scans parallel to $(h,h,0)$ performed at $l=2$, 2.15, and 2.3 are identical. Figure 4(a) shows the temperature-dependent comparison of the l-independent scatterings for the $l=3$ peak from l scans and the $l=2.15$ peak from $(hh0)$ scans. They have a similar temperature dependence, although both are normalized to the lowest temperature point, which in the case of the $l=2.15$ peak had a lower intensity and larger error, giving the apparent offset in the data. Moreover, temperature-dependent scans of $\mathbf{Q_2}=(0.71,0.71,1)$ shown in Fig. 4(b) demonstrate a similar temperature dependence on $\mathbf{Q_2}=(0.71,0.71,0)$ [Fig. 2(a)], suggesting that the spin reorientation behaves identically regardless of the magnetic Bragg reflection originating from the magnetic ridge or not. Any difference in behavior below the spin-reorientation temperature would result in a relative change in the elastic intensity between the two scans, which is not the case, meaning the spin reorientation occurs homogeneously from the l=odd Bragg reflection and the l-independent Bragg ridge. The temperature dependence of the ridge scattering and the integrated intensity of the magnetic Bragg reflections at $\mathbf{Q_1}$ and $\mathbf{Q_2}$ are consistent with the polarized-neutron data. Significantly, a weak peak is ob-

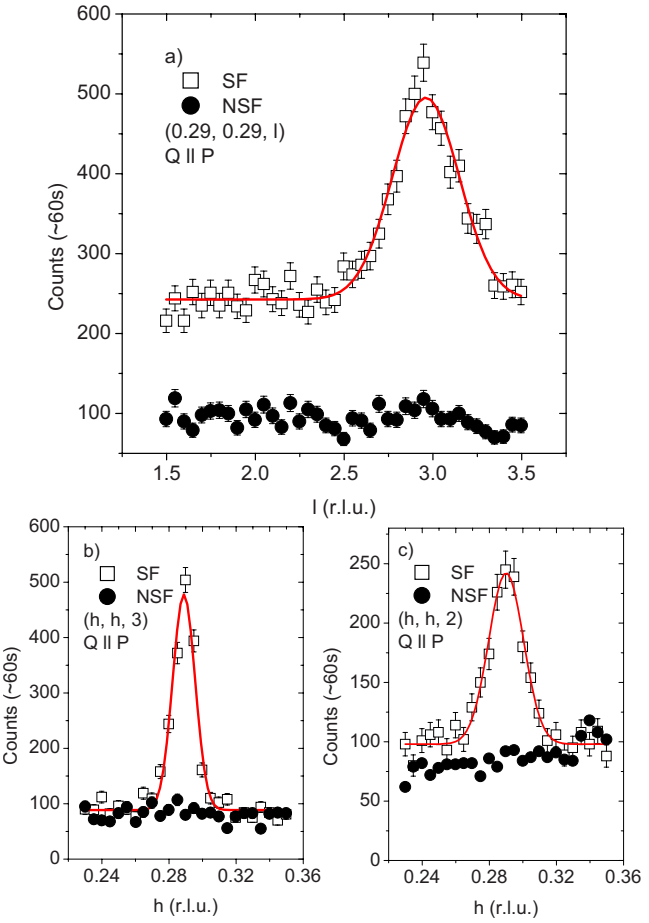

FIG. 3. (Color online) Neutron diffraction of the magnetic Bragg reflections with $\mathbf{P} \| \mathbf{Q}$ so that all SF scattering is magnetic in origin and all NSF scattering is nonmagnetic in origin. (a) A scan parallel to $(0,0,l)$ that passes through $(0.29,0.29,l)$. (b) and (c) are scans parallel to $(h,h,0)$ at $l=3$ and $l=2$, respectively. All the line shapes are Gaussian on a sloping background.

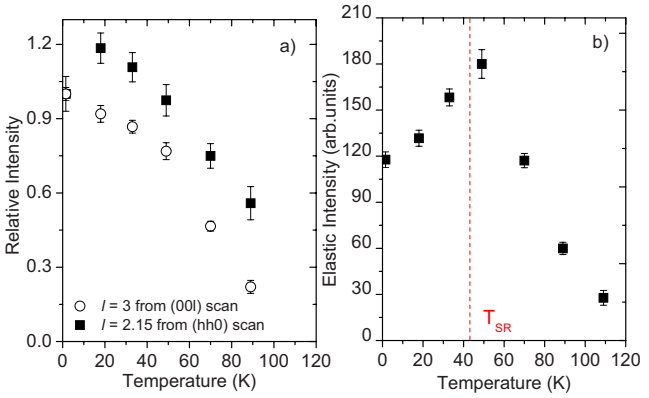

FIG. 4. (Color online) (a) Temperature dependence of the $l=3$ peak from the $(00l)$ scan compared to the temperature dependence of the $l=2.15$ from $(hh0)$ scans, showing a similar temperature dependence. (b) Temperature dependence of the intensity of the magnetic Bragg peak at $\mathbf{Q_2}=(0.71,0.71,1)$. This shows excellent agreement with Fig. 2(a).

served at $(0.58,0.58,l)$ for $l=5$ and 7, consistent with a charge-ordered peak with a correlation length on the order of 15 Å in the l direction, unlike the $x=0.5$ composition in which no l dependence is observed.[11] To enable high count rates, a neutron wave vector of $k_f=4.1$ Å^{-1} was used to significantly widen the instrument resolution so that the charge-order Bragg reflections at (1.42,1.58,0) and (1.58,1.58,0) were clearly observed on PUMA. Because of the broad resolution used, it is not possible to extract correlation lengths for these observed charge-order Bragg reflections.

The magnetic ridge that is uncorrelated along the c axis, combined with the observable peaks in Fig. 3(a) (the SF data), signifies that the magnetic order in $La_{1.55}Sr_{0.45}NiO_4$ has both 2D and 3D characters from either one magnetically ordered state or two separate magnetically ordered states. At first glance both the 2D and 3D magnetic orders have the same periodicity on the ab plane; therefore two separate magnetically ordered states seems less likely. Differentiation of these two situations is possible from a complete neutron-diffraction study of $x=0.45$, but a simpler approach is to study the internal magnetic fields using μSR. The implanted muons will have a distribution of stopping sites with respect to the spin and charge stripes, directly implying different internal fields. This will reveal itself as a volume-averaged distribution of internal fields. Therefore any impurity phase should be easily discernible by its temperature dependence. The μSR technique occupies a unique time window, $10^{-9}-10^{-6}$ s, with which to observe spin fluctuations. Indeed previous work has investigated a wide range of LSNO compositions[29–31] using μSR, observing critical behavior consistent with 2D ordering as detected via neutron-diffraction measurements. However, this work aims to explicitly combine this additional technique with bulk susceptibility and neutron diffraction upon the same crystal to reveal more information upon the local magnetic structure.

An example of a typical ZF μSR spectrum for $La_{1.55}Sr_{0.45}NiO_4$ is shown in Fig. 5(a). The data were measured at 25 K, i.e., below the ordering temperature (T_N) observed on the muon time scale. The muons were implanted

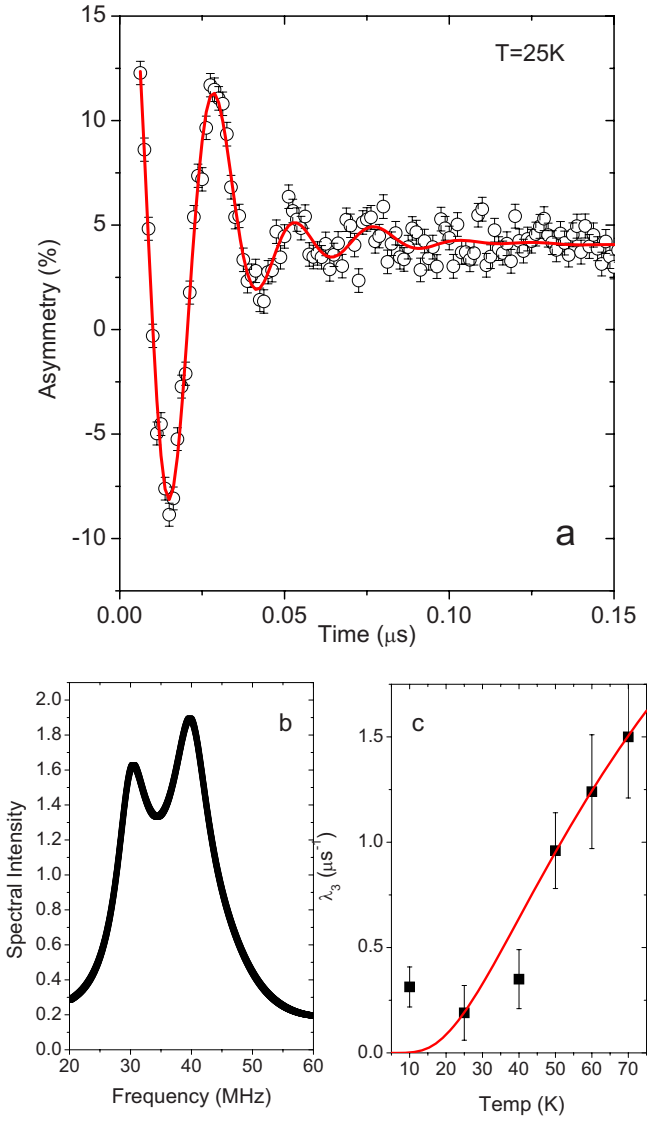

FIG. 5. (Color online) (a) ZF μSR spectra for $La_{1.55}Sr_{0.45}NiO_4$ at 25 K, along with a fit to the data by Eq. (1). Damped oscillations are clearly visible. (b) The Fourier transform of the observed oscillations. (c) The temperature dependence of the longitudinal relaxation rate together with an activated fit to the data as described in the text.

with their initial polarization perpendicular to the spins on the ab plane. The data clearly show spontaneous muon precession, observable for LSNO up to 75 K. The precessions are rapidly damped, implying a very strong relaxation. The frequency (υ_i) of the oscillations can be expressed as $\upsilon_i = \gamma_\mu |B_i|/2\pi$, where B_i is the average magnitude of the local field at the ith muon site and γ_μ is the muon gyromagnetic ratio. Any oscillatory signal observed in ZF μSR is direct evidence of long-range magnetic order. The damped oscillations could be a consequence of fluctuations of the moments surrounding the muon and/or the fact the implantation site is not unique in the unit cell of LSNO with respect to the spins and holes. Jestädt *et al.*[30] predicted a symmetrical implantation site on the NiO_2 plane. Subsequent work by Klauss[31] suggested the possibility of a muon binding to the apical

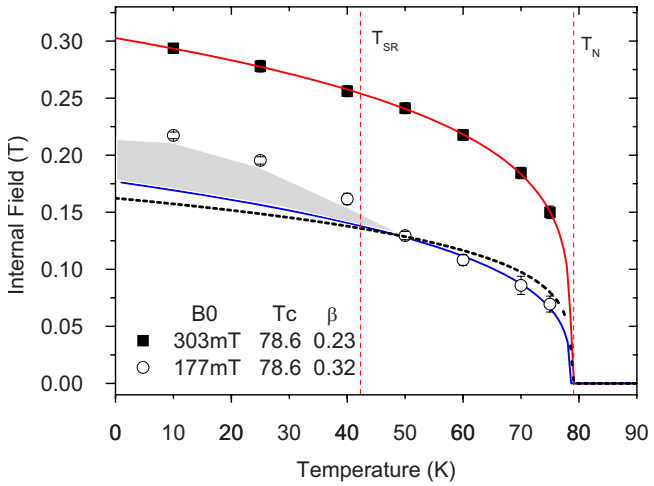

FIG. 6. (Color online) The temperature dependences of B_1 (filled squares) and B_2 (hollow circles), along with critical fits to the data as described in the text. No oscillations were observed in the ZF μSR data at 80 K. The shaded area indicates the region where the critical function no longer fits for the muons implanted into the charge stripes and indicates the observation of the SR by the muons.

oxygen to account for the large internal field distribution in LSNO relative to La_2CuO_4.

A Fourier transform of the 25 K data as shown in Fig. 5(b) indicates two distinct frequencies up to T_N in agreement with previous work performed on the $x=0.33$ sample.[31] In order to extract the temperature dependence of the two frequencies, the data can be fitted to the following function below T_N:

$$A(t) = \sum_{i=1}^{2} A_i \exp(-[\lambda_i t])\cos(2\pi \nu_i t) + A_3 \exp(-[\lambda_3 t]) + A_{\mathrm{bg}}, \tag{1}$$

where A_i represents the relative contribution for those muons undergoing coherent precession and A_3 represents the nonprecessing signal amplitude due to a local field distribution parallel to the initial spin polarization of the muon. λ is the relaxation rates for the respective components and A_{bg} represents a nonrelaxing background component from those muons which stop in the cryostat tails or the Ag sample holder. This function has been previously used to characterize the behavior of the $x=0.33$ sample.[31]

The temperature dependence of λ_3 is shown in Fig. 5(c) and clearly displays a strong reduction on decreasing the temperature below T_N. In doped transition-metal oxides, the motion of charge carriers results in a spin hopping in the opposite direction. On a local level this will give rise to a strong relaxation when the system is magnetically ordered along the direction of the initial muon polarization.[31] Moreover there is expected to be a thermally activated form of relaxation below T_N due to the charge hopping processes. Indeed λ can be described by $\lambda \propto \exp(-E_a/T)$ with $E_a = 85(10)$ K, and is shown as a fit to the data in Fig. 5(c).

The temperature evolution of $B_{i=1,2}$ is shown in Fig. 6. No oscillations were observed at temperatures higher than 75 K. During the fitting procedure all of the fitting parameters were allowed to vary; importantly the ratio of A_1 to A_2 remained constant at 4/3. The muons are randomly implanted into the material and have distinct stopping sites. Some of these sites will be close to the charge stripes, while others will be near the antiferromagnetic ordered regions, resulting in an observable volume fraction ($\equiv A$) for both the charge- and spin-stripe phases. Therefore the muons probe the local field in both the charge- and spin-ordered regions. The implantation sites of the muon enable two distinct muon precession frequencies. Although both signals are heavily damped, this can be interpreted as inequivalent magnetic regions. With the high-field (B_1) contribution as a consequence of implanted muons in the spin stripe and the lower-field (B_2) one as a result of muons situated in the charge stripes, this conclusion is in agreement with previous work on a single crystal of LSNO with a composition of $x=0.33$.[31]

The temperature dependence of the two internal field distributions (directly related to the muon precession frequency as previously described) shown in Fig. 6 displays two distinct temperature evolutions below T_N as observed by muons. To highlight this the data have been compared to a standard critical function of the form

$$B_i(T) = B_i(0)(1 - T/T_N)^{\beta}, \tag{2}$$

above 50 K, where T_N is the transition temperature and β is the critical component. When all the parameters are allowed to float for B_1, it is found that $T_N = 78.6(0.5)$ K and $\beta = 0.23(2)$. The value of β is what can be expected for a typical 2D ordered material with XY-type interactions.[32] The fit is clearly applicable down to the lowest temperature of 10 K measured in this experiment. The fit of Eq. (2) to B_2 (muons implanted into the charge stripe) is not so well defined. When T_N was 78.6 K the extracted value of β is 0.32; this is indicative of 3D Heisenberg, not 2D ordering.[32]

The data show two distinct temperature evolutions, indicative of muons implanted into the spin and charge stripes being sensitive to different magnetic regions. When the data are force fitted to have $\beta=0.23$ (dashed line) for B_2, it is clear that this value for the critical exponent does not fit the experimental data, as T_N is approached. The B_2 value of $\beta = 0.32$ is consistent with the muon being implanted into the unordered charge stripe and seeing the internal fields of neighboring ordered spins in the ab layer it is implanted in and the internal fields of neighboring ordered spins of the layers above and below the implantation site. Importantly, the onset temperatures of both $B_{1,2}$ are identical, suggesting that the observations are not simply attributable to phase separation and can be explained with an interpretation consistent with one magnetically ordered phase. This is further confirmed by the ratio of A_1:A_2 matching the spin- and charge-stripe ratio obtained using $(1-\varepsilon)/\varepsilon = 1.35 \sim 4/3$ from the neutron-scattering measurements.

IV. DISCUSSION

It is currently assumed that the charge stripe contains no ordered Ni moments.[33] Therefore the origin of the magnetic

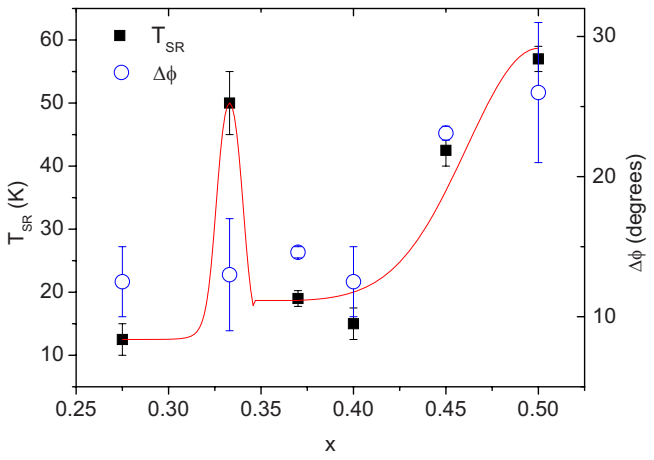

FIG. 7. (Color online) The compositional dependence of the spin-reorientation temperature (T_{SR}) and the spin-reorientation angle ($\Delta\phi$). The line is a guide for the eyes. The T_{SR} and $\Delta\phi$ are taken from Ref. 12.

order observed by the muons implanted in the charge stripe may be a direct consequence of the ordered moments in the spin stripe. This would also account for the reduced value of the internal field. Moreover the value of T_N, 78.6 K, appears to signify that static magnetic order has been achieved. This is clearly visible in the temperature dependence of the differential mass susceptibility, as shown in the inset of Fig. 1 and the observed muon oscillations. At 78 K the FC and ZFC mass susceptibility data also show irreversible behavior. This behavior is not a traditional spin glass, a process that has well-defined relaxations in ZF μSR.[34] The muons located in the charge stripe observe a three-dimensional contribution to the critical behavior. Any exchange in the c axis is very weak compared with in-plane exchange[35,36] and could explain the origin of the glassy behavior, as shown in the inset of Fig. 1.

The temperature dependence of B_2 in Fig. 6 also demonstrates a deviation from critical behavior below 50 K. Measurements in Figs. 1 and 2 have clearly demonstrated that a SR occurs at 42 K. The change in the functional form of the temperature dependence of B_2 suggests that the muons in the charge stripe are also sensitive to the SR. This is clearly highlighted as the shaded region in Fig. 6. Although previous work has discussed SR detection with muons, no work has systematically proved it with polarized-neutron studies on an identical sample.[31,37–39] Moreover the muon is acting as a passive probe of the SR as it is observing the change in spin polarization with respect to the crystal axis from the charge stripe. As the magnitude of the moment is unaltered, this also explains why no SR is seen in the muons implanted into the spin stripe.

Measurements of the SR in $x=0.45$ indicate that the enhancement of the T_{SR} and the size of the SR in $x=0.5$ (Ref. 11) is not due to a coupling to long-range checkerboard charge order. This is clearly indicated in Fig. 7, which shows the compositional dependence of T_{SR} and the spin-reorientation angle ($\Delta\phi$). This clearly demonstrates that the commensurate stripe stability that occurs at the $x=0.333$ does not occur as half doping is approached. The rotation away from the stripe direction on cooling for incommensurately doped compositions is enhanced from $10°-15°$ ($x=0.275-0.4$) to $\sim 25°$ ($x=0.45$) where the correlation length of the spin order along the c axis is on the order of 1 unit-cell length. This is unlike the enhanced T_{SR} in the $x=1/3$ which is thought to be related to commensurate pinning of the charge order to the lattice.[20] Considering the possibility of the charge stripes overlapping at higher doping, the increased T_{SR} and magnitude of the SR could be due to charge stripes being less well defined and thus having shallower potentials than separated charge stripes. If the SR reorientation is due to a competition of the ordered spins with a spin or charge degree of freedom associated with the charge stripes, then the weakening definition and hence effect of the charge stripe could enable T_{SR} and magnitude of the SR to increase.

Importantly this work observes a magnetic ridge which is two dimensional in character and signifies the possible influence of propagation along the c axis at high doping levels. Specifically in commensurate compositions, stacking along c can propagate in an ordered way along the c axis. However other incommensurate doping levels cannot, suggesting that disorder increases with doping and results in 2D scatter as observed for $x=0.45$. Such a model can describe the intensity of the magnetic Bragg reflections in charge-stripe-ordered $La_2NiO_{4+\delta}$.[40] If the charge-stripe order is commensurately spaced parallel to $(h,h,0)$, then the stripes would stack in a body-centered-tetragonal fashion, ensuring that only $l=$odd magnetic Bragg reflections are observed, as in $x=1/3$. However, incommensurate charge-stripe order will lead to nonideal stacking of the charge stripes, resulting in additional $l=$even magnetic Bragg reflections, as in $0.275 \leq x \leq 0.4$.[12,20] Moreover the correlation length of $l=$odd is twice that of the $l=$even peaks. A qualitative explanation has been proposed;[12] for $x=0.45$ the correlation length along the c axis from the $l=$odd magnetic Bragg peaks is between 1.5 and 2 unit cells long. The expected correlation length for the $l=$even peak is half that of the odd peak, less than 1 magnetic unit cell. Hence the $l=$even Bragg reflections are associated with nonideal charge-stripe stacking losing their correlation along the c axis. A possible origin of such an effect is because of the influence of strain from Sr-ion doping.

With increasing doping La^{3+} ions are replaced by the larger Sr^{2+} ions, increasing the size of the La/Sr-O layer, while holes are doped into the Ni-O layer, increasing the average Ni valency and thus reducing the size of Ni-O layer. Moreover the angle ϕ that the spins order away from lying parallel to the stripe below the spin reorientation increases with doping in the $x=0.333-0.5$ region. This trend does not match the behavior of the ordering temperatures in LSNO. Above $x \sim 0.5$ the difference in layer size prohibits large single-crystal growth, suggesting the importance of strain in the system.[10] Any distortion on the ab plane and along the c axis should be able to be probed using high-resolution x-ray diffraction.

At present a complete structural analysis of charge-stripe and spin-stripe orderings in LSNO has not been performed. This is due to the weak strength of charge-stripe Bragg reflections and the short correlation lengths of stripe order along the l direction limiting the number of observable superstructure reflections. The results of our studies however

provide an accurate account of the doping variation in the magnetic ordering, which should provide a stringent basis for theoretical models of charge-stripe order in LSNO. Along with the l dependence of the different magnetic Bragg reflections, one of the biggest remaining issues of charge-stripe order in LSNO is a theoretical description of the charge order preferentially ordering with charge stripes three Ni sites apart.[8,9] The doping dependence of LSNO $x<0.135$ is unstudied, and hence the crossover from the Néel antiferromagnet state to charge-stripe ordered. The transition to a charge-stripe-ordered state in LSNO would be insightful in understanding the same crossover to the charge-stripe-ordered state in the cuprates.[41]

The analysis and discussions are based on the generally excepted charge-ordered model of $La_{2-x}Sr_xNiO_4$. In materials such as manganates and cobaltates that are thought to be similarly charged or orbitally ordered, recent alternative models have been proposed based on neutron-diffraction measurements.[42,43] LSNO shows diverse behavior with doping, such as the l dependence of magnetic Bragg reflections and the presence of a SR reorientation with doping dependence. As such LSNO will represent a stringent test of any universal model of doped transition-metal oxides. The need to improve general theories of doped transition-metal oxides is desirable to achieve a better understanding of the doped transition-metal oxides, colossal magnetoresistance (CMR), and high-temperature superconducting materials.

V. CONCLUSIONS

In summary $La_{1.55}Sr_{0.45}NiO_4$ has been studied using neutron diffraction, μSR, and susceptibility techniques. A spin reorientation at 42 K was observed using all techniques. From neutron diffraction it was determined that, on cooling, the spins rotate $23.9\pm0.5°$ away from the stripe direction. To our knowledge only the SR in the LSNO $x=0.5$ compound has such a large SR. Moreover the large SR and the high onset temperature is observed even though the magnetic order and charge stripes are not commensurate. The neutron-diffraction work shows that the observed magnetic order is characterized by both 2D and 3D orders, indicating the importance of the spin- and charge-ordering propagations along the c axis. The muon technique suggests that the material is fully magnetically ordered. Two distinct magnetic regions were observed using muons; those implanted into the charge stripe are sensitive to the SR. The temperature dependence of the observed frequencies from μSR are consistent with the glassy magnetic transition and the neutron observations. The diverse magnetic properties of charge-ordered $La_{1.55}Sr_{0.45}NiO_4$ further add to the wealth of behavior of $La_{2-x}Sr_xNiO_4$. However the physical origin of the SR is still not understood and the consequences of determining an accurate model should have direct implications for understanding other materials demonstrating spin-stripe order.

ACKNOWLEDGMENTS

We would like to thank R. Scheuermann and R. Mole for useful discussions and experimental assistance. This research project was supported by the European Commission under the Sixth Framework Programme through the Key Action: Strengthening the European Research Area, Research Infrastructures (Contract No. RII3-CT-2003-505925).

*sean.giblin@rl.ac.uk

[1] T. R. Thurston, R. J. Birgeneau, M. A. Kastner, N. W. Preyer, G. Shirane, Y. Fujii, K. Yamada, Y. Endoh, K. Kakurai, M. Matsuda, Y. Hidaka, and T. Murakami, Phys. Rev. B **40**, 4585 (1989).

[2] S-W. Cheong, G. Aeppli, T. E. Mason, H. Mook, S. M. Hayden, P. C. Canfield, Z. Fisk, K. N. Clausen, and J. L. Martinez, Phys. Rev. Lett. **67**, 1791 (1991).

[3] J. M. Tranquada, B. J. Sternlieb, J. D. Axe, Y. Nakamura, and S. Uchida, Nature (London) **375**, 561 (1995).

[4] K. Yamada, C. H. Lee, K. Kurahashi, J. Wada, S. Wakimoto, S. Ueki, H. Kimura, Y. Endoh, S. Hosoya, G. Shirane, R. J. Birgeneau, M. Greven, M. A. Kastner, and Y. J. Kim, Phys. Rev. B **57**, 6165 (1998).

[5] S. Wakimoto, G. Shirane, Y. Endoh, K. Hirota, S. Ueki, K. Yamada, R. J. Birgeneau, M. A. Kastner, Y. S. Lee, P. M. Gehring, and S. H. Lee, Phys. Rev. B **60**, R769 (1999).

[6] C. H. Chen, S-W. Cheong, and A. S. Cooper, Phys. Rev. Lett. **71**, 2461 (1993).

[7] S. M. Hayden, G. H. Lander, J. Zarestky, P. J. Brown, C. Stassis, P. Metcalf, and J. M. Honig, Phys. Rev. Lett. **68**, 1061 (1992); V. Sachan, D. J. Buttrey, J. M. Tranquada, J. E. Lorenzo, and G. Shirane, Phys. Rev. B **51**, 12742 (1995); J. M. Tranquada, D. J. Buttrey, and V. Sachan, *ibid.* **54**, 12318 (1996).

[8] H. Yoshizawa, T. Kakeshita, R. Kajimoto, T. Tanabe, T. Katsufuji, and Y. Tokura, Phys. Rev. B **61**, R854 (2000).

[9] R. Kajimoto, T. Kakeshita, H. Yoshizawa, T. Tanabe, T. Katsufuji, and Y. Tokura, Phys. Rev. B **64**, 144432 (2001).

[10] R. Kajimoto, K. Ishizaka, H. Yoshizawa, and Y. Tokura, Phys. Rev. B **67**, 014511 (2003).

[11] P. G. Freeman, A. T. Boothroyd, D. Prabhakaran, D. González, and M. Enderle, Phys. Rev. B **66**, 212405 (2002).

[12] P. G. Freeman, A. T. Boothroyd, D. Prabhakaran, M. Enderle, and C. Niedermayer, Phys. Rev. B **70**, 024413 (2004).

[13] P. G. Freeman, A. T. Boothroyd, D. Prabhakaran, and J. Lorenzana, Phys. Rev. B **73**, 014434 (2006).

[14] E. D. Isaacs, G. Aeppli, P. Zschack, S. W. Cheong, H. Williams, and D. J. Buttrey, Phys. Rev. Lett. **72**, 3421 (1994); A. Vigliante, M. von Zimmermann, J. R. Schneider, T. Frello, N. H. Andersen, J. Madsen, D. J. Buttrey, Doon Gibbs, and J. M. Tranquada, Phys. Rev. B **56**, 8248 (1997).

[15] Yu. G. Pashkevich, V. A. Blinkin, V. P. Gnezdilov, V. V. Tsapenko, V. V. Eremenko, P. Lemmens, M. Fischer, M. Grove, G. Guntherodt, L. Degiorgi, P. Wachter, J. M. Tranquada, and D. J. Buttrey, Phys. Rev. Lett. **84**, 3919 (2000).

[16] P. D. Hatton, M. E. Ghazi, S. B. Wilkins, P. D. Spencer, D. Mannix, T. d'Almeida, p. Prabhakaran, A. T. Boothroyd, and S-W. Cheong, Physica B **318**, 289 (2002).

[17] Guoqing Wu, J. J. Neumeier, Christopher D. Ling, and Dimitri N. Argyriou, Phys. Rev. B **65**, 174113 (2002).
[18] G. Blumberg, M. V. Klein, and S-W. Cheong, Phys. Rev. Lett. **80**, 564 (1998).
[19] P. Calvani, A. Paolone, P. Dore, S. Lupi, P. Maselli, P. G. Medaglia, and S-W. Cheong, Phys. Rev. B **54**, R9592 (1996).
[20] S. H. Lee, S. W. Cheong, K. Yamada, and C. F. Majkrzak, Phys. Rev. B **63**, 060405(R) (2001).
[21] P. G. Freeman, A. T. Boothroyd, D. Prabhakaran, C. D. Frost, M. Enderle, and A. Hiess, Phys. Rev. B **71**, 174412 (2005).
[22] D. Prabhakaran, P. Isla, and A. T. Boothroyd, J. Cryst. Growth **237**, 815 (2002).
[23] J. Schmalian and P. G. Wolynes, Phys. Rev. Lett. **85**, 836 (2000).
[24] A. Aharony, R. J. Birgeneau, A. Coniglio, M. A. Kastner, and H. E. Stanley, Phys. Rev. Lett. **60**, 1330 (1988).
[25] F. C. Chou, N. R. Belk, M. A. Kastner, R. J. Birgeneau, and Amnon Aharony, Phys. Rev. Lett. **75**, 2204 (1995).
[26] J. I. Budnick, B. Chamberland, D. P. Yang, Ch. Niedermayer, A. Golnik, E. Recknagel, M. Rossmanith, and A. Weidinger, Europhys. Lett. **5**, 651 (1988).
[27] B. J. Sternlieb, G. M. Luke, Y. J. Uemura, T. M. Riseman, J. H. Brewer, P. M. Gehring, K. Yamada, Y. Hidaka, T. Murakami, T. R. Thurston, and R. J. Birgeneau, Phys. Rev. B **41**, 8866 (1990).
[28] T_{SR} in LSNO is defined as the temperature at which a reflection equivalent to $\mathbf{Q}_2$ loses intensity in neutron diffraction, and is thus an onset temperature.
[29] K. H. Chow, P. A. Pattenden, S. J. Blundell, W. Hayes, F. L. Pratt, Th. Jestädt, M. A. Green, J. E. Millburn, M. J. Rosseinsky, B. Hitti, S. R. Dunsiger, R. F. Kiefl, C. Chen, and A. J. S. Chowdhury, Phys. Rev. B **53**, R14725 (1996).
[30] Th. Jestädt, K. H. Chow, S. J. Blundell, W. Hayes, F. L. Pratt, B. W. Lovett, M. A. Green, J. E. Millburn, and M. J. Rosseinsky, Phys. Rev. B **59**, 3775 (1999).
[31] H. H. Klauss, J. Phys.: Condens. Matter **16**, S4457 (2004).
[32] S. J. Blundell, *Magnetism in Condensed Matter* (Oxford University Press, Oxford, 2001).
[33] A. T. Boothroyd, P. G. Freeman, D. Prabhakaran, A. Hiess, M. Enderle, J. Kulda, and F. Altorfer, Phys. Rev. Lett. **91**, 257201 (2003).
[34] Y. J. Uemura, T. Yamazaki, D. R. Harshman, M. Senba, and E. J. Ansaldo, Phys. Rev. B **31**, 546 (1985).
[35] A. T. Boothroyd, D. Prabhakaran, P. G. Freeman, S. J. S. Lister, M. Enderle, A. Hiess, and J. Kulda, Phys. Rev. B **67**, 100407(R) (2003).
[36] Y. Oohara, R. Kajimoto, T. Kakeshita, H. Yoshizawa, T. Tanabe, T. Katsufuji, K. Ishizaka, Y. Taguchi, and Y. Tokura, Physica B **329-333**, 725 (2003).
[37] L. P. Le, G. M. Luke, B. J. Sternlieb, Y. J. Uemura, J. H. Brewer, T. M. Riseman, D. C. Johnston, and L. L. Miller, Phys. Rev. B **42**, 2182 (1990).
[38] G. M. Luke, L. P. Le, B. J. Sternlieb, Y. J. Uemura, J. H. Brewer, R. Kadono, R. F. Kiefl, S. R. Kreitzman, T. M. Riseman, C. E. Stronach, M. R. Davis, S. Uchida, H. Takagi, Y. Tokura, Y. Hidaka, T. Murakami, J. Gopalakrishnan, A. W. Sleight, M. A. Subramanian, E. A. Early, J. T. Markert, M. B. Maple, and C. L. Seaman, Phys. Rev. B **42**, 7981 (1990).
[39] P. Mendels, D. Bono, J. Bobroff, G. Collin, D. Colson, N. Blanchard, H. Alloul, I. Mukhamedshin, F. Bert, A. Amato, and A. D. Hillier, Phys. Rev. Lett. **94**, 136403 (2005).
[40] P. Wochner, J. M. Tranquada, D. J. Buttrey, and V. Sachan, Phys. Rev. B **57**, 1066 (1998).
[41] M. Matsuda, M. Fujita, K. Yamada, R. J. Birgeneau, Y. Endoh, and G. Shirane, Phys. Rev. B **65**, 134515 (2002).
[42] A. Daoud-Aladine, J. Rodriguez-Carvajal, L. Pinsard-Gaudart, M. T. Fernandez-Diaz, and A. Revcolevschi, Phys. Rev. Lett. **89**, 097205 (2002).
[43] A. T. Savici, I. A. Zaliznyak, G. D. Gu, and R. Erwin, Phys. Rev. B **75**, 184443 (2007).